Arabian Journal for Science and Engineering (2019) 44:2103–2113
https://doi.org/10.1007/s13369-018-3346-4

RESEARCH ARTICLE - ELECTRICAL ENGINEERING

Switching Control Paradigms for Adaptive Cruise Control System with Stop-and-Go Scenario

Z. Haroon[1] · B. Khan[1] · U. Farid[1] · S. M. Ali[1] · C. A. Mehmood[1]

Received: 19 August 2017 / Accepted: 22 May 2018 / Published online: 5 June 2018

Abstract
The adaptive cruise control (ACC) system is currently one of the most common research topics in automotive industry. The ACC system tracks the velocity of preceding vehicle by adjusting the throttle angle and applying brake, whenever needed. This system is acknowledged for improving the fuel efficiency due to coordination between brake and throttle. Inappropriate switching between brake and throttle results in loss of energy that increases fuel consumption. To address aforesaid problem, novel coordinated switching controllers for the ACC system are proposed that enhances the fuel efficiency. Moreover, the proposed control strategies are compared for various traffic scenarios, and then, fuel economy is observed for the proposed control schemes. Fuel economy is investigated using switching control paradigm design; namely, the proportional–integral–derivative (PID) controller, adaptive proportional–integral–derivative (APID) controller, and fuzzy PID controller for actual nonlinear and linearized model of the ACC system for various traffic scenarios including stop and proposed control strategies are compared using performance indices for various traffic scenarios, such as CC, ACC, and ACC stop and go in order to show the validity of the design. Furthermore, the comparison among the PID, APID, and fuzzy PID control schemes is investigated to analyze fuel economy of the actual nonlinear CC and ACC system.

Keywords Adaptive cruise control (ACC) · Adaptive proportional integral derivative (APID) · Fuel economy · Fuzzy PID · Proportional integral derivative (PID) · Stop and go (SG)

1 Introduction

Safety and energy are two basic concerns of the automotive industry. The energy crisis is growing worst nowadays. The anticipation of energy crisis avoids the future era of expensive and limited energy. Maximum fuel consumption, environmental deterioration, and transport congestion are severe problems caused in urban areas with increasing transportation demands [1]. Large population, shortage of public transport system, rapid growth in private vehicles, low investment in infrastructure, and poor parking policies are the foremost reasons of traffic jam in developing countries [2]. The human errors and accidents are caused because of driver's frustration in traffic congestion. The adaptive cruise control (ACC) system is an automatic driver assistance system that improves driver's comfort and road safety under disturbances [3]. The ACC system has two modes of operation: (a) cruise control (CC) mode and (b) ACC mode. The CC mode of operation is active when road is clear, and ACC-equipped vehicle follows the driver's set speed. The CC mode fails to detect the preceding vehicle. The ACC mode of operation is used to incorporate data of the preceding vehicle. The ACC system made a very vital impact on society by changing the way of life because of the following: (a) reduces driver fatigue, (b) improves traffic efficiency, (c) increases convenience and productivity, (d) minimizes fuel economy, (e) less impact on environment, and (f) more safety.

In an ACC system, appropriate switching between brake and throttle is vital. The frequent switching affects the perfor-

✉ Z. Haroon
zubaidaharoon@ciit.net.pk

B. Khan
bilalkhan@ciit.net.pk

U. Farid
umarfarid@ciit.net.pk

S. M. Ali
hallianali@ciit.net.pk

C. A. Mehmood
chaudhry@ciit.net.pk

[1] Department of Electrical Engineering, COMSATS Institute of Information Technology, Abbottabad 22060, Pakistan

mance of the cascaded control (as inner-loop control (ILC) and outer-loop control (OLC) are two cascaded control loops, and disturbance in OLC loop has critical impact on the performance of the ILC), increases fuel consumption, and damages vehicle components. Considering above, there is a pressing need to design control schemes that incorporates coordinated and optimal operation of throttle and brake.

Various control schemes were developed in the literature for an appropriate switching between brake and throttle. Automotive industry uses various control schemes that varies from conventional PID [4] to the most sophisticated nonlinear control schemes [5–7] such as sliding mode control [8–11], fuzzy logic [12,13], and neural network [14,15] for improving reference speed tracking of the ACC-equipped vehicle.

In [16], the PI-based CC mode was used in passenger car for achieving required speed. The PI control scheme used trial-and-error method to handle alterations in plant and thus fails to incorporate varying conditions. The authors in [17] designed trial ACC model with hybrid PID to develop the ACC stop and go (ACCSG) in passenger car for avoiding accidents in urban areas. The trial ACC model included control of inter-vehicle gap management system and monitors movement of other vehicles. The change in reference speed produced oscillations and required time to smooth out. The gain scheduling proportional integral (GSPI) and gain scheduling linear quadratic (GSLQ) were used for various linear models of the throttle [18]. The aforesaid linear models were extracted for various operating points. The PI control scheme was used for brake. The GSPI proved good performance for the CC mode. In the ACC mode, GSPI and GSLQ showed good performance for the proposed ACC system. The control schemes failed in situation of stop and go.

In [19], the authors used the fuzzy logic-based ACC system to assure safe car following by controlling brake pressure and throttle angle. Although safety was observed, the fuzzy logic fails as oscillations that affect driver's comfort were present. The fuzzy PID control scheme was used for switching paradigm in the ACC system for improving fluctuations, thus providing comfortable driving [20]. The fuzzy PID control scheme lacks the incorporation of the fuel economy. The engine operating in an idle speed minimizes fuel consumption, during coasting phase fuel must be cut off from the engine [21,22].

The aforementioned literature is extended for designing PID, APID, and fuzzy PID control schemes for various traffic scenarios that includes CC, ACC, and ACCSG. The performance indices (PIs) of all proposed control schemes are considered for attaining an optimal control strategy. The switching paradigms designed in this paper are further used for achieving the fuel efficiency.

The main contributions of our paper for switching control paradigms for ACC with stop-and-go scenario in light of above-stated issues are:

- Nonlinear and linear models of the ACC are presented for the analysis of an appropriate switching controller that effects the fuel consumption;
- The PID, APID, and fuzzy PID control schemes are designed for various traffic scenarios, and proposed control schemes are compared for achieving the best switching control paradigm;
- PIs are calculated for the evaluation of the system's performance by means of various proposed control schemes; and
- The fuel consumption for the CC, ACC, and ACCSG using PID, APID, and fuzzy PID control schemes is compared for achieving best optimal control strategy that incorporates fuel efficiency.

The paper is structured as follows: Sect. 2 presents detailed nonlinear modeling of the ACC system. The linear modeling of the ACC system is provided in Sect. 3. The proposed APID and fuzzy PID control design for the ACC system is elaborated in Sect. 4. The comparison of PID, APID, and fuzzy PID control schemes for observing tracking of reference speed is presented in Sect. 5. The results achieved for fuel economy of proposed control schemes are illustrated in Sect. 6. The paper concludes with a brief summary and proposed future work.

2 ACC System Modeling

The ACC system is an extension of the CC system that relies on the automatic adjustment between the brake and throttle [23]. The ACC system uses two control loops: (a) inner-loop control (ILC) and (b) outer-loop control (OLC) [24]. The OLC collects information of the preceding vehicle, i.e., the distance between two vehicles d, the vehicle's velocity v_h, and acceleration. The ILC receives information from the OLC. The OLC ensues the information using vision system with lidar system and radar system [25,27]. The constant time headway (CTH) policy maintains specific distance between the two vehicles, i.e., approximately 1.5–2 s [28]. The block diagram of the ACC system is presented in Fig. 1.

The vehicle model utilized for the development of the ACC system design considers the longitudinal motion of the vehicle.

According to the Newton's second law of motion:

$$F_{\text{net}} = \text{ma}. \tag{1}$$

where F_{net} is the sum of forces, m represents mass of vehicle in kg and a is used for acceleration.

$$F_{\text{net}} = F_{\text{wheel}} + F_{\text{aeroD}} + F_{\text{rollingF}} + F_{\text{g}}. \tag{2}$$

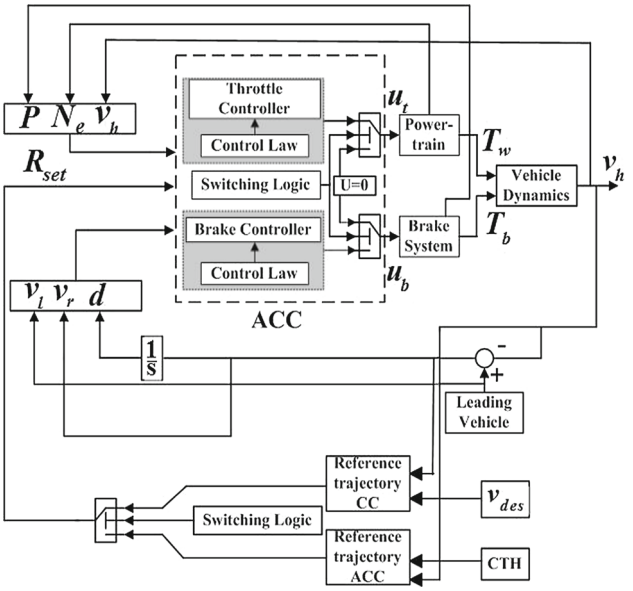

Fig. 1 Block diagram of the ACC model

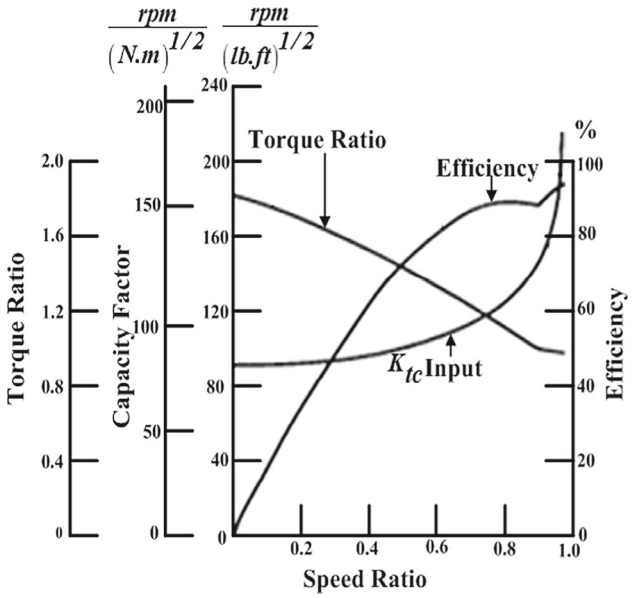

Fig. 2 Performance characteristic of a torque converter [29]

In Eq. (2), F_{wheel} is the force applied on wheel, F_{aeroD} represents the aerodynamic drag force, F_{rollingF} is used for the rolling friction, and F_{g} is the gravitational force.

The velocity of the host vehicle is formulated as:

$$\dot{V}_h = \frac{1}{m}\left[\begin{array}{l}\frac{1}{r}\left[R_{\text{tr}}R_{\text{fd}}C_{\text{tr}}\left(\frac{N_e}{K_{\text{tc}}}\right)^2 + T_{\text{b}}\right] - \\ \frac{1}{2}\rho A C_d v_h^2 - C_r mg\cos\theta + mg\sin\theta\end{array}\right], \tag{3}$$

where R_{tr} is the gear Ratio, R_{fd}denotes the final drive ratio, N_{e} represents the engine speed in rad/sec, T_{b} is used for the braking torque, $\frac{1}{2}\rho A C_d v_h^2$ is the coefficient of the aerodynamic drag, C_{r} denotes the coefficient of rolling resistance, m represents the total vehicle mass, g is known gravity acceleration, and θ is the road slope. The torque ratio is represented as C_{r} and calculated from Fig. 2.

The torque of engine is calculated by using relation as:

$$I_{ei}\dot{N}_{\text{e}} = T_{\text{e}}(u_{\text{t}}, N_{\text{e}}) - T_{\text{i}}. \tag{4}$$

The engine speed in [30] is rewritten as:

$$\dot{N}_{\text{e}} = \frac{1}{I_{\text{ei}}}\left[T_{\text{ei}}(u_t, N_{\text{e}}) - T_{\text{f}} - T_{\text{p}} - \left(\frac{N_{\text{e}}}{K_{\text{tc}}}\right)^2\right] \tag{5}$$

In Eq. (5), K_{tc} is the capacity factor that is calculated from graph in Fig. 3.

$T_{\text{i}} = \left(\frac{N_{\text{e}}}{K_{\text{tc}}}\right)^2$ is the impeller torque (acting load), T_{f} represents the engine friction loss, and T_{p} is the engine pumping losses.

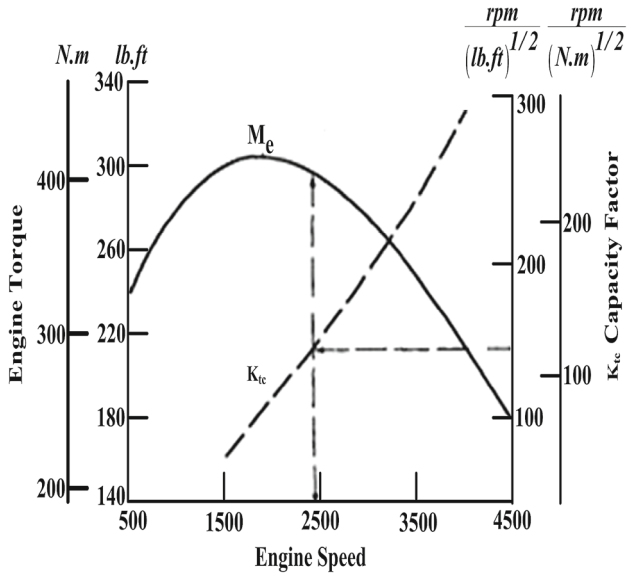

Fig. 3 Capacity factor of an internal combustion engine [29]

The engine impeller torque is a function of throttle signal and engine speed $T_{\text{ei}}(u_{\text{t}}, N_{\text{e}})$. The engine map is presented in Fig. 4.

The front and rear wheels have different braking torques due to the load transfer during braking. The brake model in [32] is formulated as:

$$P_{\text{bj}} = 150K_{\text{cj}}u_{\text{bj}} - \tau_{\text{bs}}\dot{P}_{\text{bj}}, \quad \forall j = (r, f) \tag{6}$$

The pressure applied on brake disk is written as:

$$\dot{P}_{\text{bj}} = \frac{150K_{\text{cj}}u_{\text{bj}} - \tau_{\text{bs}}\dot{P}_{\text{bj}}}{\tau_{\text{bs}}}. \tag{7}$$

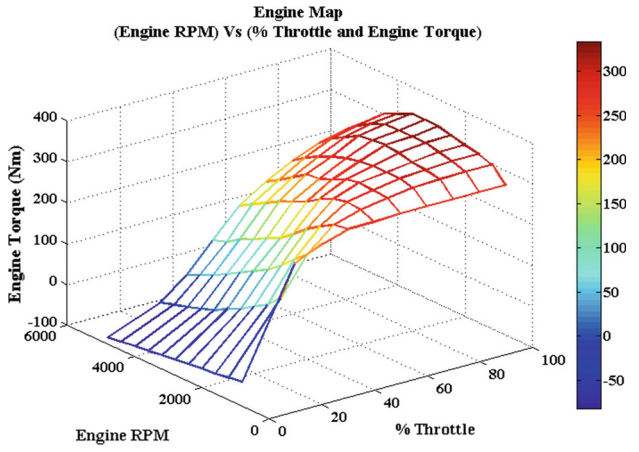

Fig. 4 Engine map for T_{ei} as a function of N_e for various fixed values of u_t is throttle input [31]

In Eq. (7), τ_{bs} is the lumped lag-servo valve and the hydraulic system, K_c denotes the pressure gain, u_b is the brake input, and P_b represents the pressure behind brake disk (Its range is from 0 to 150 bar).

In the ACC system, leading vehicle acts as disturbance; hence, $\dot{v}_l$ is assumed as: 0 The ACC system is also known as "distance tracking control". The distance is calculated by taking integral of the relative velocity for assuring safety between two vehicles. The relation between distance and relative velocity is described in [30]. Therefore, we can write the expression for distance as:

$$\dot{d} = v_{rel} = v_l - v_h. \tag{8}$$

v_l is the velocity of preceding vehicle and v_h represents the host vehicle velocity.

3 Linearization of the ACC System

The ACC system model developed in Sect. 2 is for the nonlinear system. This section covers the linearization of the actual nonlinear ACC system to get simplification in terms of controlling the ACC system. in the ACC system, nonlinearity arises in the ILC that consists of brake and throttle. The ILC is linearized for different operating points. Steps of linearizing the ILC are elaborated in Sect. 3.1, while general form of the state-space equation is discussed in detail in Sect. 3.2.

3.1 Steps of Linearization

Throttle and brake contribute the nonlinearity of the ACC system. The steps of linearizing the ACC system are as follows:

(1) Throttle is active when brake is inactive.
(2) Brake is active when throttle is inactive.

3.2 State-Space Model of the ACC System

The general form of state-space equation is:

$$\dot{\mathbf{x}}(\mathbf{t}) = \mathbf{A}x(t) + \mathbf{B}u(t), \tag{9}$$

$$\mathbf{y}(\mathbf{t}) = \mathbf{C}x(t) + \mathbf{D}u(t). \tag{10}$$

In Eqs. (9) and (10), $x(t) \in R^n$, $y(t) \in R^p$, and $u(t) \in R^m$, where n denotes the number of states, m represents the number of inputs, and p is the number of outputs.

The state-space model of actual nonlinear ACC system is formulated in Eqs. (9) and (10). The aforementioned linearization of ILC is attained for two operating points, i.e., throttle and brake [31]. The nonlinear states of ACC model are presented as

$$x = \begin{bmatrix} P & v_h & N_e & v_l & d \end{bmatrix}^T \tag{11}$$

After linearization and removal of redundant states in Eqn. (11) using two operating points (throttle active $u_b = 0$, break inactive and break active $u_t = 0$, throttle inactive) may be rewritten as:

$$x = [v_h \quad N_e]^T. \tag{12}$$

The numerical values of the state-space equations for brake and throttle are presented in "Appendix".

4 Controller Design

4.1 APID Control Scheme

The backpropagation (BP) algorithm is used for designing the APID controller. The APID complete system is divided into four parts. The first three parts of controller are k_p, k_i, and k_d, whereas controlled plant is the fourth part. The closed-loop feedback control system is depicted in Fig. 5. The BP algorithm uses the gradient descent function which is defined as:

$$J = \frac{1}{2}e^2, \tag{13}$$

$$J = \frac{1}{2}(v_h - v_{ref})^2. \tag{14}$$

In Eq. (14), v_h is the velocity of host vehicle (also known as following vehicle in case of the ACC system) and v_{ref} is the reference velocity.

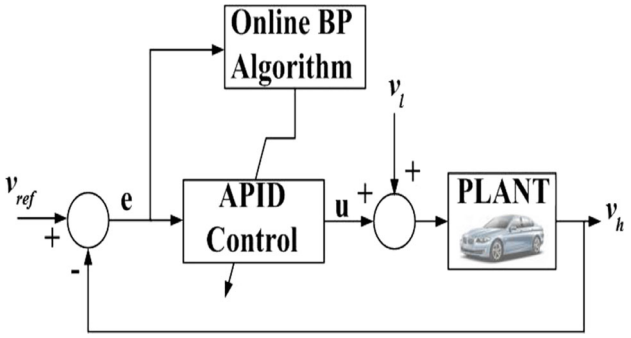

Fig. 5 Structure of adaptive PID controller for the ACC system

The BP algorithm's gain is calculated as:

$$\dot{k} = -\gamma \frac{dJ}{dk}, \tag{15}$$

In Eq. (15), $k \in \{k_p, k_i, k_d\}$ where k_p, k_i, and k_d represent the proportional, integral, and derivative parameters of the controller and γ is the learning rate where $\gamma \in (0\ 1)$.

4.1.1 Learning Parameters

The BP optimization is used for minimizing the cost function and to speed up the convergence. The updated parameters and learning procedure are calculated as:

$$\dot{k}_{\mathrm{p}} = -\gamma \frac{\partial J}{\partial y}\frac{\partial y}{\partial u}\frac{\partial u}{\partial k_p}, \tag{16}$$

$$\dot{k}_i = -\gamma \frac{\partial J}{\partial y}\frac{\partial y}{\partial u}\frac{\partial u}{\partial k_{\mathrm{i}}}, \tag{17}$$

$$\dot{k}_{\mathrm{d}} = -\gamma \frac{\partial J}{\partial y}\frac{\partial y}{\partial u}\frac{\partial u}{\partial k_d}. \tag{18}$$

where $y = v_{\mathrm{h}}$ and $u = v_{\mathrm{ref}}$

Equations (16), (17), and (18) are rewritten as:

$$\dot{k}_p = -\gamma e x_1, \tag{19}$$

$$\dot{k}_i = -\gamma e x_2. \tag{20}$$

$$\dot{k}_d = -\gamma e x_3. \tag{21}$$

where x_1, x_2, and x_3 are inputs for k_p, k_i, and k_d, respectively, and error is denoted by e. The desired updated values of k_p, k_i, and k_d are formulated as:

$$k_{\mathrm{p}}(t+1) = k_{\mathrm{p}}(t) + \dot{k}_{\mathrm{p}}(t), \tag{22}$$

$$k_{\mathrm{i}}(t+1) = k_{\mathrm{i}}(t) + \dot{k}_{\mathrm{i}}(t), \tag{23}$$

$$k_{\mathrm{d}}(t+1) = k_{\mathrm{i}}(t) + \dot{k}_{\mathrm{d}}(t). \tag{24}$$

The learning rate is used for the convergence of the BP algorithm. The APID control scheme is tuned online based on the BP algorithm. In the closed-loop system, the updated parameters of the APID are used for minimizing error and speed up the convergence of the system.

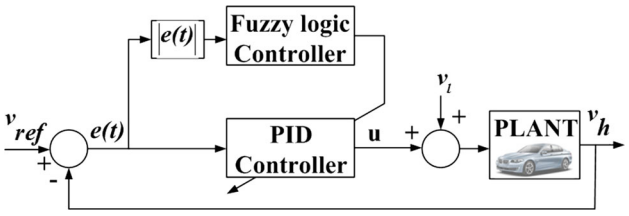

Fig. 6 Closed-loop structure of the fuzzy PID control scheme for the ACC system

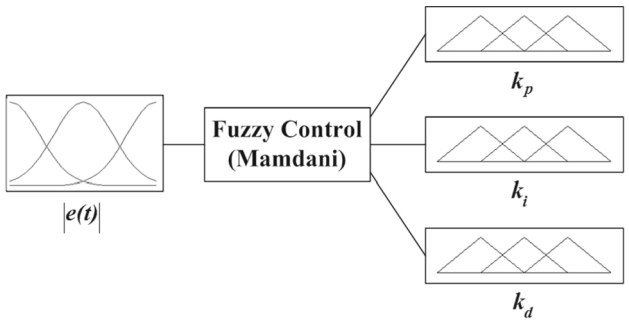

Fig. 7 Fuzzy inference block

4.2 Fuzzy PID Control Scheme

The fuzzy PID control scheme is developed for improving the performance of the ACC system as presented in Fig. 6. The fuzzy PID control integrates the advantages of PID and fuzzy control scheme. The membership function used in fuzzy PID structure is of Gaussian. Center-of-sums technique is used for deffuzzification.

The tuning parameters are obtained from Mamdani model that is for fuzzy inference system (FIS). The FIS block diagram is presented in Fig. 7. The absolute of error is the input of FIS, and k_p , k_i , and k_d are three outputs. The fuzzy PID control scheme improves driving safety of the ACC system, achieves smaller oscillations, and manages comfortable traveling.

The variable ranges of the PID controller are supposed as $[k_{p\ \min}, k_{p\ \max}]$, $[k_{i\ \min}, k_{i\ \max}]$, and $[k_{d\ \min}, k_{d\ \max}]$, respectively. The simulation of PID control scheme determines the range of each parameter. For calibration of PID parameter ranges, intervals used are: $k_p \in [10, 100]$, $k_i \in [0.1, 1]$, and $k_d \in [0.001, 0.01]$ as presented in [33]. Therefore, the updated parameters are calculated as:

$$\dot{k}_p = \frac{k_p - k_{p\ \min}}{k_{p\ \max} - k_{p\ \min}} = \frac{k_p - 10}{100 - 10}, \tag{25}$$

$$\dot{k}_i = \frac{k_i - k_{i\ \min}}{k_{i\ \max} - k_{i\ \min}} = \frac{k_i - 0.1}{1 - 0.1}, \tag{26}$$

Table 1 Fuzzy inference rules

Rule number	Fuzzy rules
1	If $\|e(t)\| = 0$, then k_p=L and k_i=S and k_d=0
2	If $\|e(t)\| = S$, then k_p=L and k_i=0 and k_d=0
3	If $\|e(t)\| = L$, then k_p=L and k_i=L and k_d=0

S: small, L: large, Z: zero

$$\dot{k}_d = \frac{k_d - k_{d\ \min}}{k_{d\ \max} - k_{d\ \min}} = \frac{k_d - 0.001}{0.01 - 0.001}. \tag{27}$$

The parameters of PID control scheme are updated online via fuzzy rules given in Table 1. Gaussian and triangular membership functions are used in antecedent and consequent part, respectively, for updating of fuzzy rules. Antecedent part of the fuzzy system is absolute error, and the consequent part is the tuned values of PID, i.e., k_p, k_i, and k_d. The fuzzy PID parameters are adopted and updated online using fuzzy inference rules in Table 1.

Therefore, updated gains are k_p, k_i, and k_d may be calculated from Eqs. (25), (26), and (27) as:

$$k_p = 90\dot{k}_p + 10, \tag{28}$$

$$k_i = 0.9\dot{k}_i + 0.1, \tag{29}$$

$$k_d = 0.009\dot{k}_d + 0.001. \tag{30}$$

The tuning parameters k_p, k_i, and k_d improve system performance specifications such as steady-state error, rise time, overshoot, and settling time.

5 Performance Evaluation

Our objective is to reduce driver burden, increase the traffic flow output, improve safety, increase fuel efficiency, and decrease traffic accidents using various control schemes for the ACC system. The proposed control schemes include: (a) PID (Ziegler–Nichols method is used for PID tuning), (b) APID, and (c) fuzzy PID design for different traffic scenarios. All control schemes are compared for linear and nonlinear ACC model to illustrate the best switching control paradigm for the brake and throttle. The proposed control schemes are compared through computer simulations using MATLAB/Simulin$_k$.

The system's sensitivity and precision are tested for various PIs. The PI calculations are used for achieving an appropriate and beneficial control scheme for the specified system. The computational cost of control scheme is linked with accuracy and imprecision for each control algorithm. The decision on control law selection for the system is based on PI response of each control paradigm. Some commonly used PIs in practice are integral square error (ISE), integral of the absolute magnitude of error (IAE), and integral time-square error (ITSE) where ISE, IAE, and ITSE mathematically are defined as: ISE $= \int_0^t |e(t)|\,\mathrm{d}t$, IAE $= \int_0^\infty t\,|e(t)|\,\mathrm{d}t$, and ITSE $= \int_0^t |e^2(t)|\,\mathrm{d}t$, respectively. Performance indices are calculated in pu-sec.

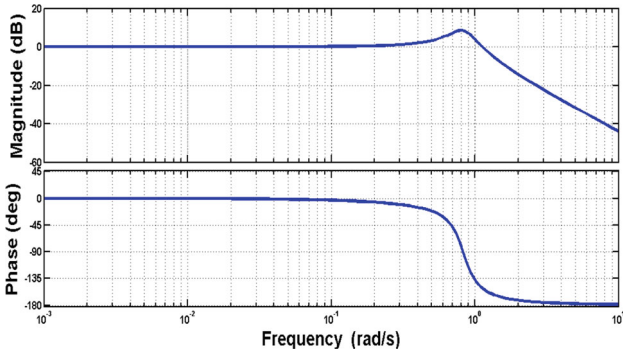

Fig. 8 Bode plot for the ILC

The closed-loop transfer function of CC system is:

$$\frac{v_h(s)}{v_t(s)} = \frac{0.637s + 0.0098}{s^3 + 0.4657s^2 + 0.002485s} \tag{31}$$

Bode diagram for the transfer function is sketched in Fig. 8. The bandwidth frequency is calculated for the ILC and OLC. Bandwidth frequency is the frequency corresponding to the closed-loop magnitude response at -3dB. The large bandwidth can pass higher frequencies more easily; hence, large bandwidth corresponds to a faster rise time. Figure 8 illustrates the bandwidth of the CC system approximately equals to 1.24 rad/s (0.19735Hz). The ILC has faster response, as higher bandwidth frequency is observed.

The transfer function of the OLC is:

$$\begin{aligned}\frac{v_h(s)}{v_{rel}(s)} &= \frac{0.637s^4+0.9432s^3+0.3124s^2+0.006225s+0.02522}{s^6+1.695s^5+1.565s^4+1.111s^3+0.3132s^2+0.006224s+0.02522} \\ &\times \frac{0.637s^4+0.9432s^3+0.3124s^2+0.006225s+2.522e^{-05}}{s^6+1.695s^5+1.565s^4+1.111s^3+0.3132s^2+0.006224s+2.522e^{-05}}.\end{aligned} \tag{32}$$

The bode diagram for Eq. (32) is presented in Fig. 9. The bandwidth frequency observed for OLC is 0.8821 rad/s (0.1404 Hz). The bandwidth of the OLC is lower than the ILC.

The minimum bandwidth shows that the response time of the OLC is slower than ILC.

The ACC system is a cascaded network that consists of the ILC and OLC, where disturbance in the OLC causes malfunctioning in ILC. Considering above, the response time of the ILC should always be greater than the OLC. The proper synchronization between the ILC and OLC is observed.

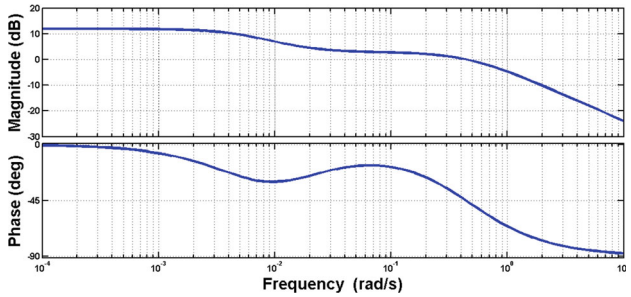

Fig. 9 Bode plot for the OLC

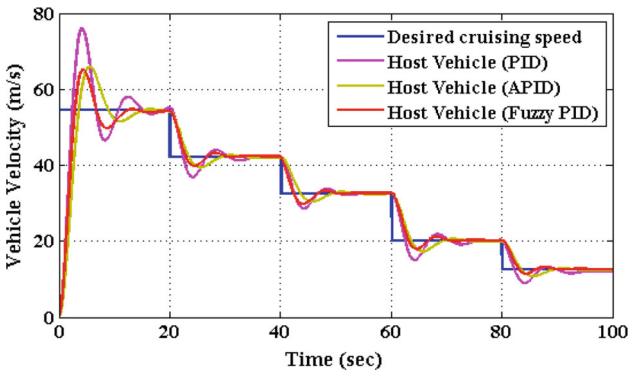

Fig. 10 The system operates in CC mode (linear model)

Table 2 PI quantitative values for the Linear CC system

Control scheme	Performance indices			
	ISE	IAE	ITAE	ITSE
PID	1.449×10^4	606.7	6.067×10^4	1.449×10^6
APID	9613	393.7	3.937×10^4	9.613×10^5
Fuzzy PID	4263	229.9	2.299×10^4	4.263×10^5

Comparison of the proposed control schemes for the linear CC system is presented in Fig. 10. When system operates in the CC mode, no vehicle is present in front of the host vehicle, and desired cruising speed is followed that is the driver's set speed. The desired cruising speed varies for various intervals. Figure 10 demonstrates that PID control overshoot is greater at the beginning and then settles down at 17 s. However, the APID controller oscillates for 18 s and the fluctuation for fuzzy PID control scheme is minimum. The fuzzy PID control technique improves the fuel efficiency, driving safety, and passenger comfort.

In case of the linear CC system, the quantitative values of the PI for ISE, IAE, ITAE, and ITSE are presented in Table 2 for all proposed control paradigms. The control scheme with minimum PI is considered as an optimal control scheme. The fuzzy PID control scheme is approved as fuel efficient among all control schemes.

Figure 11 shows the comparison of all proposed control paradigms for nonlinear CC system, as performance differs

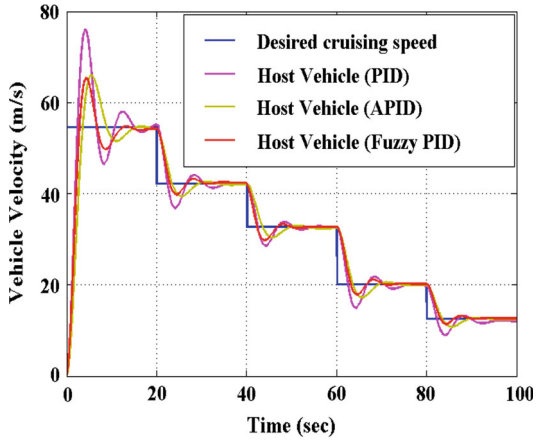

Fig. 11 The system operates in the CC mode (nonlinear model)

Table 3 PI quantitative values for the nonlinear CC system

Control scheme	Performance indices			
	ISE	IAE	ITAE	ITSE
PID	1.116×10^5	2322	2.322×10^5	1.116×10^7
APID	1.819×10^4	659.2	6.592×10^4	1.819×10^6
Fuzzy PID	0.382×10^2	532	9.32×10^2	0.592×10^5

for each control scheme. In the beginning, the PID control has overshoot of 74.5%. Overshoot causes system instability that affects passenger comfort and fuel consumption. Transients in the PID control settle down at 18 s; thus, the desired cruising speed is attained after a long duration. The APID has ability of adapting values in accordance with the variation in system parameters. Therefore, the desired cruising speed is adapted earlier than conventional PID control. The comparison of the PID, APID, and fuzzy PID control schemes indicates that the fuzzy PID has no overshoot and steady-state error. Therefore, the comfortable driving is achieved.

The performance comparison of proposed control paradigms for nonlinear CC system in Table 3 illustrates the optimum system with fuzzy PID.

In Fig. 12, as the ACC-equipped vehicle detects the leading vehicle, the ACC mode becomes active. The host vehicle starts following the leading vehicle instead of desired cruising speed that is set by the driver. When ACC mode is active, PID, APID, and fuzzy PID control schemes are designed so that the host vehicle follows the velocity of the leading vehicle. The APID control scheme starts tracing the velocity of leading vehicle at 37 s. The simulation results of the fuzzy PID control scheme are best as safe following of leading vehicle is observed and safe distance between two vehicles, i.e., the leading and the host vehicle is maintained.

Proposed control paradigms for linear ACC system are demonstrated in Table 4 for various PI quantitative values such as ISE, IAE, ITAE, and ITSE. As fuzzy PID improves

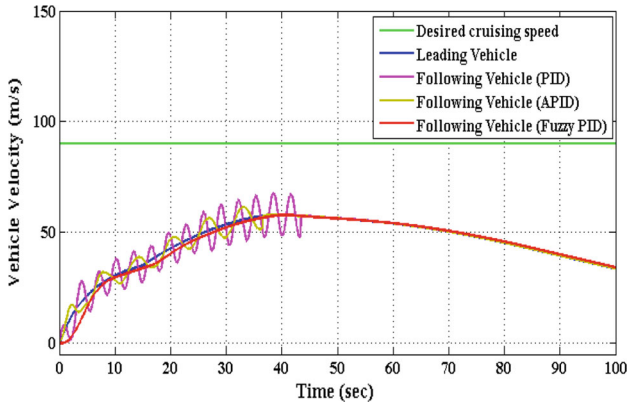

Fig. 12 The system operates in the ACC mode (linear model)

Table 4 PI quantitative values for the linear ACC system

Control scheme	Performance indices			
	ISE	IAE	ITAE	ITSE
PID	3808	262.3	2.623×10^4	3.808×10^5
APID	2586	305.5	3.055×10^4	2.586×10^5
Fuzzy PID	1326	409.3	4.65×10^3	1.432×10^4

the performance of the ACC system, therefore minimum PI is observed.

The switching control paradigms such as PID, APID, and fuzzy PID are compared in Fig. 11 for the actual nonlinear ACC system. The PID control scheme starts following the velocity of leading vehicle at 78 s, while the APID control follows at 62 s. The fuzzy PID control scheme designed for the actual nonlinear ACC system exhibits considerable improved system performance.

The fuzzy PID control results in appropriate switching between brake and throttle. The APID control scheme compared with PID improves the performance of the nonlinear ACC system. The comparison of PID, APID, and fuzzy PID in Fig. 13 is further clarified in Table 5. The table illustrates that the fuzzy PID control scheme has best performance, as PI for the fuzzy PID control scheme presents the smaller value.

The ACCSG is extension of the ACC system, covering range of 0–58 m/s. Initially leading vehicle accelerates to 58 m/s; at 25 s, it decelerates to 6 m/s and then increases the velocity. The control schemes are developed independently for brake and throttle. The comparison of proposed control schemes is presented in Fig. 14. In case of PID control, the following vehicle starts following the velocity of leading vehicle after 11 s, and oscillations are also observed. During stop-and-go condition that is shown in the interval between 25 and 63 s, the APID control scheme starts following the leading vehicle earlier than the PID control. The ACCSG simulation results proved that the fuzzy PID control

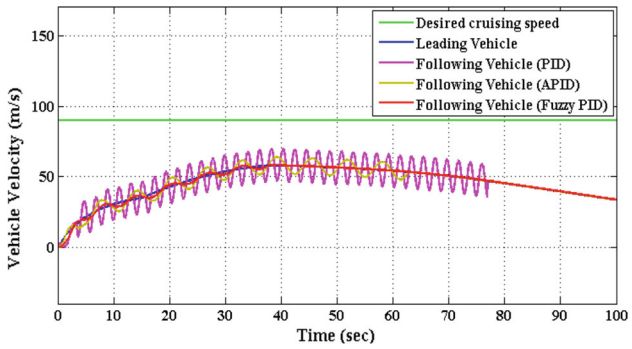

Fig. 13 The system operates in the ACC mode (nonlinear model)

Table 5 PI quantitative values for the nonlinear ACC system

Control scheme	Performance indices			
	ISE	IAE	ITAE	ITSE
PID	1.075×10^5	2236	2.236×10^5	1.075×10^7
APID	8025	498.4	4.984×10^4	8.025×10^5
Fuzzy PID	6451	389.5	4.671×10^3	6.053×10^4

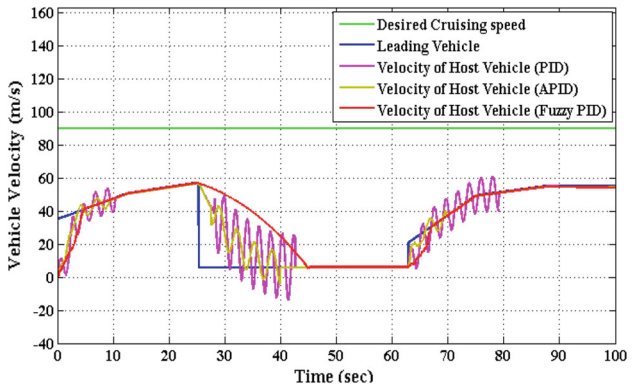

Fig. 14 The linear ACCSG system

Table 6 PI quantitative values for the linear ACCSG system

Control scheme	Performance indices			
	ISE	IAE	ITAE	ITSE
PID	3808	262.3	2.623×10^4	3.808×10^5
APID	2586	305.5	3.055×10^4	2.586×10^5
Fuzzy PID	1935	282.5	$4.6.1 \times 10^4$	1.873×10^4

scheme results in smooth switching between brake and throttle, thus providing improved results for the ACCSG system.

The simulation results of Fig. 12 are organized in Table 6. The PI for the fuzzy PID control scheme presents minimum value, as system performance is increased with suitable rising and settling time.

Simulation results of control paradigms such as PID, APID, and fuzzy PID for the actual nonlinear ACCSG system

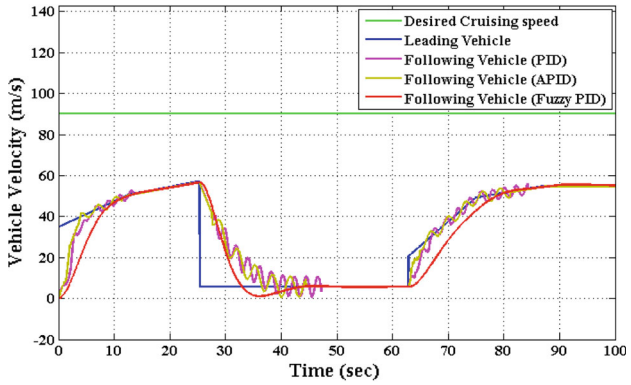

Fig. 15 The nonlinear ACCSG system

Table 7 PI quantitative values for the nonlinear ACCSG system

Control scheme	Performance indices			
	ISE	IAE	ITAE	ITSE
PID	5990	321.7	3.217×10^4	5.99×10^5
APID	4571	285.9	2.859×10^4	4.571×10^5
Fuzzy PID	3910	201.4	7.058×10^3	6.513×10^4

are shown in Fig. 15. The APID control scheme has fewer oscillations as compared with the conventional PID control, thus following the velocity of the leading vehicle precisely. The fuzzy PID control scheme has no overshoot, and stability is observed for the nonlinear ACCSG system that increases traveling comfort and fuel efficiency.

The fuzzy PID control scheme has appropriate rising and settling time that results in increased performance of the ACCSG system. The PI quantitative values for ISE, IAE, ITAE, and ITSE are compared in Table 7 for proposed control paradigms for linear CC system. The minimum PI of the fuzzy PID control scheme shows improved performance.

6 Fuel Economy

In today's world, the modern automotive engineering focused on reduction in fuel consumption. The different control schemes are used for increasing fuel efficiency. In this regard, the comparison of PID, APID, and fuzzy PID control schemes is compared for various traffic scenarios.

Table 8 presents values for the CC mode of operation using the PID, APID, and fuzzy PID control schemes. The fuzzy PID control illustrates much efficient results as compared with PID and APID control schemes.

Simulation results for the ACC system are presented in Table 9. The fuzzy PID control scheme improves fuel saving, as fuel consumption decreases with an increase in stability.

Table 8 Fuel economy for CC nonlinear model

Quantity	Control scheme		
	PID	APID	Fuzzy PID
Liter/100 km	11.59	11.55	11.26
km/l	8.629	8.659	9.098
MPG (miles per gallon)	20.3	20.37	20.89
Total fuel used (l)	0.4492	0.4486	0.3412

Table 9 Fuel economy for ACC nonlinear model

Quantity	Control scheme		
	PID	APID	Fuzzy PID
Liter/100 km	12.49	12.45	11.98
km/l	8.004	8.03	9.36
MPG (miles per gallon)	18.89	18.83	19.34
Total fuel used (l)	0.5645	0.5626	0.4932

Table 10 Fuel economy for nonlinear ACCSG System

Quantity	Control scheme		
	PID	APID	Fuzzy PID
Liter/100 km	22.45	22.15	20.08
km/l	15.034	15.04	16.05
MPG (miles per gallon)	23.78	23.89	24.09
Total fuel used (l)	3.457	3.4552	3.0512

The APID control scheme is fuel efficient as compared with the conventional PID control.

The ACCGG depicts the fuel economy for proposed control schemes in Table 10. The ACC system with fuzzy PID control scheme covers distance of 9.36 km with 1 l; APID utilizes 1 liter for 8.03 km, while the total distance covered with the integration of the PID control scheme is 9.36 km. The fuzzy PID improves fuel efficiency for ACCSG scenario.

7 Conclusion and Future Work

The incorporation of fuel economy data plays a pivotal role in designing the ACC system. The system stability, passenger comfort, and fuel economy, a control designer must incorporate various switching control paradigms considering all possible traffic scenarios. We analyzed the effect of proposed control paradigms for various traffic scenarios such as CC, ACC, and ACCSG considering fuel efficiency for each scenario. We analyzed that the fuzzy PID control scheme is efficient for both linear and nonlinear models of the ACC system.

Our future work will consider electric vehicle power consumption for numerous control schemes. Recent work covers various PID control schemes such as conventional PID, APID, and fuzzy PID. Advance nonlinear control schemes are able to improve the ACC system performance and fuel consumption, so future work will look on model predictive control (MPC) and hybrid MPC (HMPC).

8 Appendix

The state-space representation for throttle is:

$$\mathbf{A}_t = \begin{bmatrix} -0.0054 & 0.0001 \\ 0.0059 & -0.4603 \end{bmatrix}, \tag{8.1}$$

$$\mathbf{B}_t = \begin{bmatrix} 0 \\ 686.2546 \end{bmatrix}, \tag{8.2}$$

$$\mathbf{C} = \begin{bmatrix} 0.0714 & 0 \end{bmatrix}, \tag{8.3}$$

$$\mathbf{D} = 0. \tag{8.4}$$

When brake is active and throttle is inactive, state-space model for brake is obtained as:

$$\mathbf{A}_b = \begin{bmatrix} -0.0056 & 0.0001 \\ 0.0050 & -0.4597 \end{bmatrix}, \tag{8.5}$$

$$\mathbf{B}_b = \begin{bmatrix} -0.0827 \\ 0 \end{bmatrix}, \tag{8.6}$$

$$\mathbf{C} = \begin{bmatrix} 0.0714 & 0 \end{bmatrix}, \tag{8.7}$$

$$\mathbf{D} = 0 \tag{8.8}$$

References

1. Metz, B.; Davidson, O.; Martens, J.-W.; Rooijen, S.V.; Mcgrory, L.V.W.: Methodological and Technological Issues in Technology Transfer. Cambridge University Press, Cambridge (2000)
2. Sperling, D.; Clausen, E.: The Developing World's Motorization Challenge. University of California Transportation Center, Berkeley (2002)
3. Bin, Y.; Li., K; Feng, N.: Modelling and Nonlinear Robust Control of Longitudinal Vehicle Advanced ACC Systems. In: Bartoszewicz, A. (ed.) Challenges and Paradigms in Applied Robust Control. pp. 113-146. ISBN (2011)
4. Guvenc, B.A.; Kural, E.: Adaptive cruise control simulator: a low-cost, multiple-driver-in-the-loop simulator. IEEE Control Syst. **26**(3), 42–55 (2006)
5. Aguilar-Ibañez, C.: Stabilization of the pvtol aircraft based on a sliding mode and a saturation function. Int. J. Robust Nonlinear Control **27**, 843–859 (2017)
6. Rubio, J.J.: Robust feedback linearization for nonlinear processes control. ISA Trans. (2018). https://doi.org/10.1016/j.isatra.2018.01.017
7. Aguilar-Ibanez, C.; Sira-Ramirez, H.; Suarez-Castanon, M.S.: A linear active disturbance rejection control for a ball and rigid triangle system. Math. Prob. Eng. **2016**, 1–11 (2016)
8. Naranjo, J.E.; Gonzalez, C.; Reviejo, J.; Garcia, R.; de Pedro, T.: Adaptive fuzzy control for inter-vehicle gap keeping. IEEE Trans. Intell. Transp. Syst. **4**(3), 132–142 (2003)
9. Ganji, B.; Kouzani, Z.A.; Khoo, S.Y.; Shams-Zahraei, M.: Adaptive cruise control of a HEV using sliding mode control. Exp. Syst. Appl. Int. J. **41**(2), 607–615 (2014)
10. Rubio, J.J.; Soriano, E.; Juarez, C.F.; Pacheco, J.: Sliding mode regulator for the perturbations attenuation in two tank plants. IEEE Access **5**(1), 20504–20511 (2017)
11. Jesús, R.: Sliding mode control of robotic arms with deadzone. IET Control Theory Appl. **11**(8), 1214–1221 (2017)
12. Hassan, A.; Collier, G.: Mechatronics 2013. Adaptive Cruise Control for a Robotic Vehicle Using Fuzzy Logic. Springer, Cham (2014)
13. Thanok, S.; Parnichkun, M.: Adaptive cruise control of a passenger car using hybridof sliding mode control and fuzzy logic control. In: Paper presented at the international conference on automotive engineering (ICAE-8), Thailand
14. Desjardins, C.; Chaib-draa, B.: Cooperative adaptive cruise control: a reinforcement learning approach. IEEE Trans. Intell. Transp. Syst. **12**(4), 1248–1260 (2011)
15. Cherian, M.; Sathiyan, S.P.: Neural Network based ACC for optimized safety and comfort. Int. J. Comput. Appl. (IJCA) **42**(14), 0975–8887 (2012)
16. Deka, J.; Haloi, R.: Study of effect of P, PI controller on car cruise control system and security. Int. J. Adv. Res. Electr. Electron. Instrum. Eng. (IJAREEIE) **3**(6), 9817–9822 (2014)
17. Sivaji, V.V.; Sailaja, D.M.: Adaptive cruise control systems for vehicle modeling using stop and go manoeuvres. Int. J. Eng. Res. Appl. (IJERA) **3**(4), 2453–2456 (2013)
18. Shakouri, P.; Ordys, A.; Laila, D.S; Askari, M.: Adaptive cruise control system:comparing gain-scheduling PI and LQ controllers. In: International federation of automatic control (IFAC), Milano, Italy, August 28–September 2 (2011)
19. Ko, S.-J.; KAISTz D.; Lee, J.-J.: Fuzzy logic based adaptive cruise control with guaranteed string stability. In: Paper presented at the international conference on control, automation and systems, 2007. ICCAS '07, Seoul 17–20 October (2007)
20. Gong, L.; Luo, L.; Wang, H.; Liu, H.: Adaptive cruise control design based on fuzzy-PID. In: Paper presented at the international conference on E-product E-service and E-entertainment (ICEEE), 2010, Henan, 7–9 Nov (2010)
21. Shakouri, P.; Ordys, A.; Darnell, P.; Kavanagh, P.: Fuel efficiency by coasting in the vehicle. Int. J. Veh. Technol. **2013**, 14 (2013)
22. Lee, J.: Vehicle Inertia Impact on Fuel Consumption of Conventional and Hybrid Electric Vehicle Using Acceleration and Coast Driving Strategy. Virgina Polytechnic Institute and State University, Blacksburg (2009)
23. Rajamani, R.: Vehicle Dynamics and Control. Mechanical Engineering Series. Springer, New York (2006)
24. Payman, S.; Andrzej, O.: Nonlinear model predictive control approach in design of adaptive cruise control with automated switching to cruise control. Control Eng. Pract. **26**, 160–177 (2014)
25. Fossati, A.; Schonmann, P.; Fua, P.: Real-time vehicle tracking for driving assistance. Mach. Vis. Appl. **22**, 439–448 (2011)
26. Karnfelt, C.; Peden, A.; Bazzi, A.; El Haj Shhade, G.: 77 GHz ACC radar simulation platform. In: Paper presented at the intelligent transport systems telecommunications (ITST), Lille 20–22 Oct
27. Hofmann, P.: Object Detection and Tracking with Side Cameras and Radar in an Automotive Context. Free University of Berlin, Berlin (2013)
28. Martinez, J.-J.; Canudas-de-Wit, C.: A safe longitudinal control for adaptive cruise control and stop-and-go scenarios control systems technology. IEEE Trans. **15**(2), 246–258 (2007)
29. Wong, J.Y.: Theory of Ground Vehicles, 3rd edn. Wiley, New York (2001)

30. Ma, R.; Kaber, D.B.: Situation awareness and workload in driving while using adaptive cruise control and a cell phone. Int. J. Ind. Ergon. **35**, 939–953 (2005)
31. Shakouri, P.: Designing of the Adaptive Cruise Control System-Switching Controller. Kingston University London, London (2012)
32. Short, M.; Pont, J.M.; Huang, Q.: Safety and reliability of distributed embeded systems. In: University of Leicester, Embedded systems laboratory (2004)
33. Zulfatman,; Rahmat, M.F.: Application of self-tuning fuzzy PID controller on industrial hydraulic actuator using system identification approach. Int. J. Smart Sens. Intell. Syst. **2**(2), 246–261 (2009)